

A new mathematical formulation for remote sensing of soil moisture based on the Red-NIR space

Hassan Foroughi , Abd Ali Naseri , Saeed Boroomand Nasab , Saeid Hamzeh , Morteza Sadeghi , Markus Tuller & Scott B. Jones

To cite this article: Hassan Foroughi , Abd Ali Naseri , Saeed Boroomand Nasab , Saeid Hamzeh , Morteza Sadeghi , Markus Tuller & Scott B. Jones (2020) A new mathematical formulation for remote sensing of soil moisture based on the Red-NIR space, International Journal of Remote Sensing, 41:20, 8034-8047

To link to this article: <https://doi.org/10.1080/01431161.2020.1770365>



Published online: 15 Aug 2020.



Submit your article to this journal [↗](#)



View related articles [↗](#)



View Crossmark data [↗](#)



A new mathematical formulation for remote sensing of soil moisture based on the Red-NIR space

Hassan Foroughi^{a,b}, Abd Ali Naseri^a, Saeed Boroomand Nasab^a, Saeid Hamzeh^c,
Morteza Sadeghi^d, Markus Tuller^e and Scott B. Jones^b

^aDepartment of Irrigation and Drainage, Shahid Chamran University of Ahvaz, Ahvaz, Iran; ^bDepartment of Plants, Soils, and Climate, Utah State University, Logan, UT, USA; ^cDepartment of Remote Sensing and GIS, Tehran University, Tehran, Iran; ^dDepartment of Civil, Environmental & Geo-Engineering, University of Minnesota, Minneapolis, MN, USA; ^eDepartment of Environmental Science, The University of Arizona, Tucson, AZ, USA

ABSTRACT

Optical remote sensing of earth surface processes commonly relies on the red, green, blue (RGB), near-infrared (NIR) and shortwave-infrared (SWIR) electromagnetic bands. Most of the optical sensors mounted on unmanned aerial vehicles and satellites provide the RGB and NIR bands, but only a few offer SWIR output. The Red-NIR reflectance space has been widely applied for remote sensing of various land surface variables including soil moisture. The linear relationship between the Red-NIR reflectance of bare soil is established as the base and then moisture isolines are assumed perpendicular to the soil line. In this study, we show that this assumption is not consistent with the actual Red-NIR space geometry, which in many cases introduces soil moisture estimation errors. To overcome this limitation, we propose a new mathematical transformation to the original Red-NIR space followed by newly defined soil moisture isolines that are more consistent with the actual observations. This new Transformed Red-NIR (TRN) model is compared with the Conventional Red-NIR (CRN) model using data from a sugarcane field located in southwestern Iran. Twelve Land Remote-Sensing Satellite (Landsat)-8 images were acquired during the sugarcane growth season. For validation of the remotely sensed data, ground reference soil moisture was determined at 22 locations at five different depths via core sampling and oven-drying. Our results indicate that the TRN model significantly improves the accuracy of remotely sensed soil moisture.

ARTICLE HISTORY

Received 8 August 2019
Accepted 18 February 2020

1. Introduction

Soil moisture is an important state variable that controls many ecohydrological and biogeochemical processes (Robinson et al. 2008; Babaeian et al. 2019a) and provides valuable information about subsurface water storage variations (Crow et al. 2017; Sadeghi et al. 2019). Today, remote sensing (RS) technology provides extensive geospatial soil moisture monitoring capabilities. Microwave remote sensing is the most promising

approach to soil moisture retrieval on a global scale (Kerr et al. 2001; Entekhabi et al. 2010). At smaller scales, thermal and optical RS techniques have shown great potential for high-resolution (centimetre to metre scale) mapping of soil moisture (Hassan-Esfahani et al. 2015; Babaeian et al. 2018, 2019b; Mananze, Pôças, and Cunha 2019).

Thermal RS techniques capitalize on the strong correlation between land surface temperature (LST) and soil moisture. The thermal triangle/trapezoid model is the most common thermal RS approach (Carlson, Gillies, and Perry 1994; Moran et al. 1994; Shafian and Maas 2015; Sun 2015). However, this model is not applicable for satellites lacking the thermal band (e.g. Sentinel-2). In addition, because LST depends on atmospheric variables besides soil moisture, this model requires time-consuming and computationally demanding individual calibrations for each observation date (Sadeghi et al. 2017). To overcome these limitations, Sadeghi et al. (2017) proposed replacing LST with shortwave infrared (SWIR) transformed reflectance (STR) based on an established physical linear relationship between soil moisture and STR (Sadeghi, Jones, and Philpot 2015).

Although the SWIR optical signal is the most sensitive to soil moisture variations, there are a number of RS platforms including Spot1-6, GeoEye, Ikonos, Skysat1-2, or the recently launched VENμS satellite, that do not provide SWIR observations. Furthermore, most of the unmanned aerial vehicle (UAV) mounted cameras for rapidly growing precision agriculture applications (e.g. MicaSense RedEdge and Parrot Sequoia) only provide visible band observations. These limitations have provided the motivation for development of an easy-to-apply and reasonably accurate model for RS of soil moisture based on visible (red, green, blue) and near-infrared (NIR) electromagnetic bands.

The Red-NIR space concept was first introduced by Richardson and Wiegand (1977). Ghulam et al. (2007) and Zhan et al. (2007) implemented the Red-NIR space for soil moisture estimation, based on the fact that soil reflectance decreases distinctly with increasing soil moisture in the NIR domain due to the strong absorption by water molecules. Thereafter, other researchers used the Red-NIR space for remote sensing of soil moisture (Ghulam et al. 2008; Yin et al. 2013; Amani et al. 2016; Mobasheri and Amani 2016; Chen, He, and Zhang 2017).

For modelling soil moisture based on the Red-NIR space, a 'soil line' describing the linear relationship between red and NIR reflectance of bare soil is determined and then soil moisture isolines are assumed as parallel lines perpendicular to the soil line. There are two major limitations in the conventional mathematical formulation of the Red-NIR method. The first limitation is the non-uniqueness of the soil line for large areas due to the inclusion of various soil types that can lead to uncertainties in determination of the soil line. The second limitation is that the presumed 'parallel' soil moisture isolines are not consistent with the physics of radiative transfer in soil and plant canopy. This is clearly indicated by numerical simulations of Atzberger and Richter (2012) (see their Figure 3) and analytical derivations by Taniguchi, Obata, and Yoshioka (2014, 2016), which show that the isolines are non-parallel crossing curves rather than parallel lines.

In this study, we propose a new mathematical formulation that resolves both above-mentioned limitations associated with the Conventional Red-NIR (CRN) space model. No soil line is required for the new model. The newly defined soil moisture isolines are quadratic rather than linear, which is more consistent with observations in the Red-NIR space.

2. Theoretical background

2.1. Conventional Red-NIR (CRN) model

The pixel distribution within the CRN space generally forms a curved triangular geometry as shown in Figure 1, where line CB is the soil line, the data periphery forming curve AB is the dry edge, and the data border between points A and C is the wet edge. For estimating soil moisture based on this geometry, Ghulam et al. (2007) and Zhan et al. (2007) assumed soil moisture isolines perpendicular to the soil line, as depicted in Figure 1. In the CRN model, the soil line is defined as

$$R_{\text{NIR}} = I + M \times R_{\text{Red}} \quad (1)$$

where R_{Red} is the red band reflectance, R_{NIR} is the NIR band reflectance, and M and I are the slope and intercept of the soil line, respectively.

The soil moisture isoline that meets the origin and is perpendicular to the soil line is defined as

$$R_{\text{NIR}} = I - M^{-1} \times R_{\text{Red}} \quad (2)$$

The isoline distances from line L intersecting the origin and perpendicular with the soil line are assumed to be correlated with soil moisture and calculated as follows:

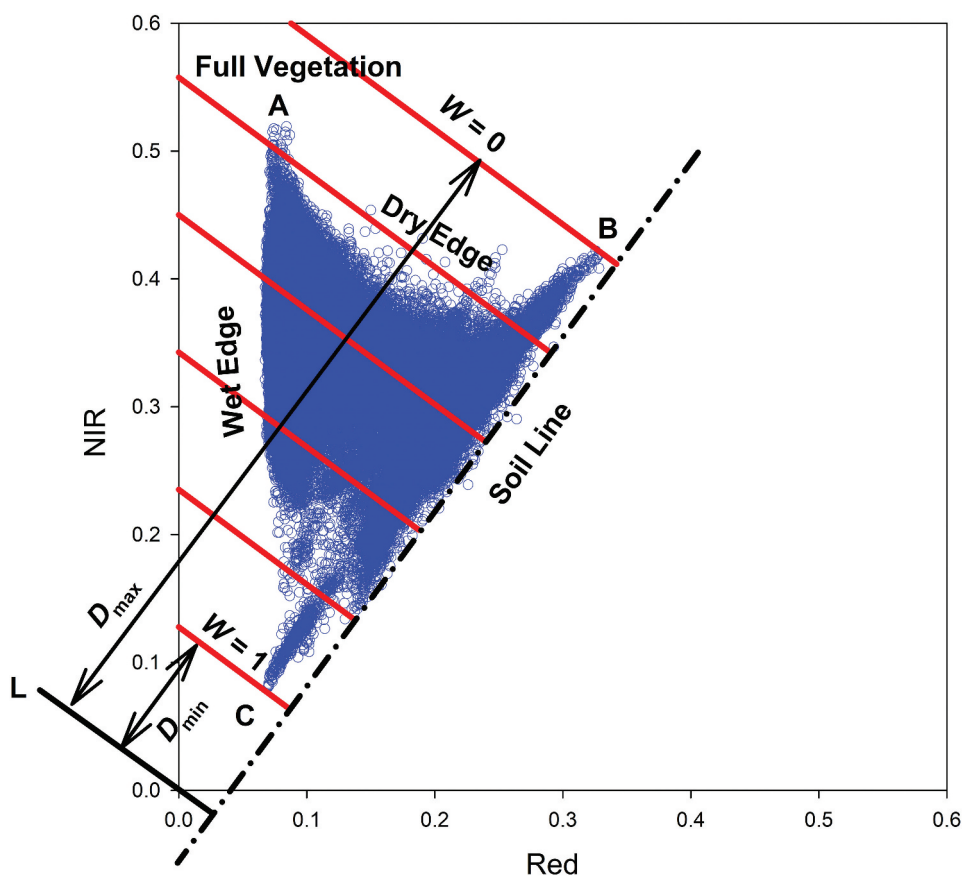


Figure 1. The conventional Red-NIR model for estimation of soil moisture (after Ghulam et al. 2007; Zhan et al. 2007). Dots are observations and red solid lines are presumed soil moisture isolines.

$$D = \frac{1}{\sqrt{M^2 + 1}} (R_{\text{NIR}} + M \times R_{\text{Red}}) \quad (3)$$

Finally, the distance D is normalized based on its maximum (D_{max}) and minimum (D_{min}) values corresponding to the isolines at points B and C in Figure 1, respectively, which yields soil saturation degree, W , as follows:

$$W = \frac{D_{\text{max}} - D}{D_{\text{max}} - D_{\text{min}}} \quad (4)$$

As shown in Figure 1, the presumed $W = 0$ and $W = 1$ isolines significantly differ from the actual dry and wet edges (i.e. AB and AC curves, respectively). With our proposed new formulation, we aim to minimize these deviations (i.e. better fit $W = 0$ to the dry edge and $W = 1$ to the wet edge) and generate isolines that better represent the actual geometry.

2.2. Transformed Red-NIR (TRN) model

As depicted in Figure 1, the dry and wet edges in the Red-NIR space have two distinct characteristics. First, both are nearly quadratic. Second, they meet each other at the full vegetation cover point (A). Therefore, we assume that all soil moisture isolines are quadratic and converge at the full vegetation cover point. Due to the fact that red reflectance decreases and NIR reflectance increases with increasing fractional vegetation cover, we characterize the full vegetation cover point based on the maximum NIR reflectance and the minimum red reflectance as

$$A = \begin{bmatrix} \text{Red}_{\text{min}} \\ \text{NIR}_{\text{max}} \end{bmatrix} \quad (5)$$

The first step of the new model, termed 'Transformed Red-NIR' (TRN) model, entails transformation of the original coordinate system such that the full vegetation cover point, A, is the origin of the new coordinate system. In the second step, the x and y axes are switched to overlay the x axis with the wet edge. This means that the red and NIR reflectance axes are first rotated by 90° counter-clockwise, and then they are shifted towards the new x - and y -direction by NIR_{max} and $-\text{Red}_{\text{min}}$, respectively. As a result, the following coordinates are obtained for the new space:

$$\begin{bmatrix} x \\ y \end{bmatrix} = \begin{bmatrix} \text{NIR}_{\text{max}} - \text{NIR} \\ \text{Red} - \text{Red}_{\text{min}} \end{bmatrix} \quad (6)$$

As illustrated in Figure 2, the following quadratic function represents soil moisture isolines that all converge at the full vegetation cover point in the new coordinate system:

$$y = ax^2 \quad (7)$$

Combining Equations (6) and (7), the parameter a can be calculated as follows:

$$a = \frac{\text{Red} - \text{Red}_{\text{min}}}{(\text{NIR}_{\text{max}} - \text{NIR})^2} \quad (8)$$

As shown in Figure 2, the newly defined soil moisture isolines match the wet ($a = 0$) and dry edges ($a = a_{\text{max}}$) much better than in the CRN method. Therefore, the parameter a provides a measure for soil moisture status, as it decreases with increasing soil moisture. A normalized soil moisture, W , can be defined as

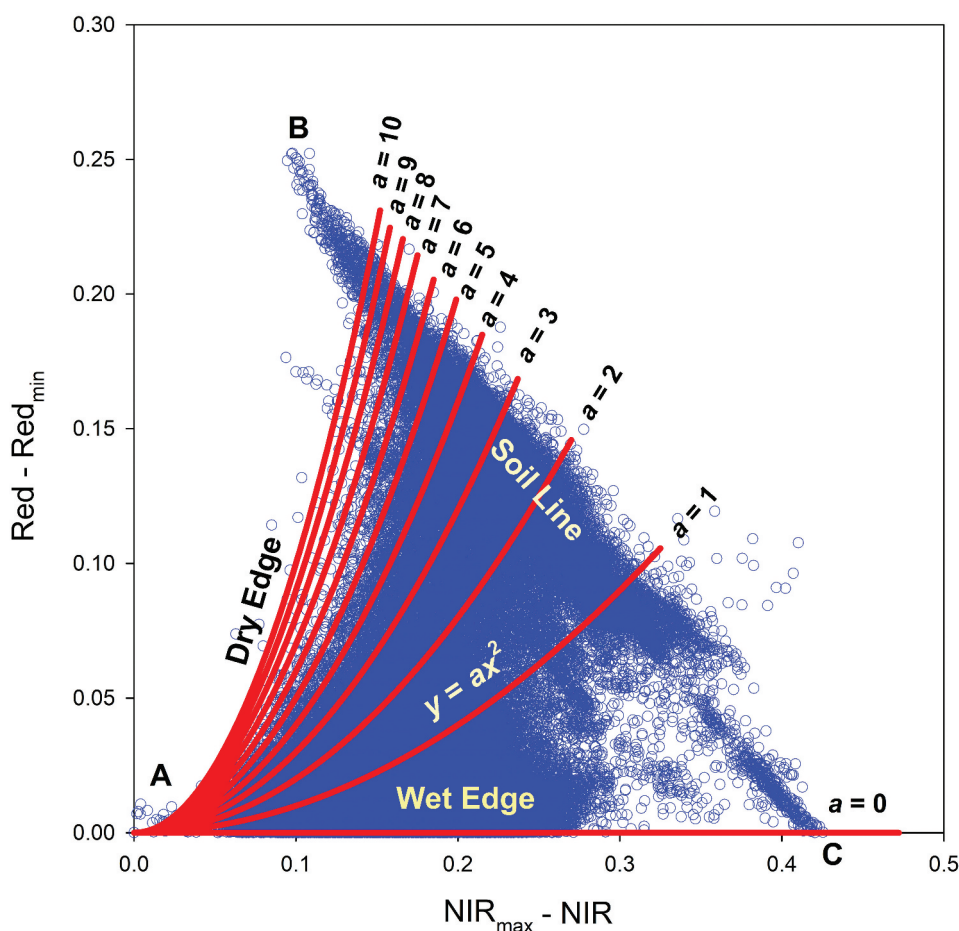


Figure 2. The proposed Red-NIR model for estimation of soil moisture. The blue dots are actual observations and the red solid lines are presumed soil moisture isolines.

$$W = 1 - \frac{a}{a_{\max}} \quad (9)$$

or

$$W = 1 - \frac{\left[\frac{\text{Red} - \text{Red}_{\min}}{(\text{NIR} - \text{NIR}_{\max})^2} \right]}{\left[\frac{\text{Red} - \text{Red}_{\min}}{(\text{NIR} - \text{NIR}_{\max})^2} \right]_{\max}} \quad (10)$$

As apparent from Equation (10), the normalized soil moisture can be straightforwardly calculated for any random point within the TRN space without the need for determining the soil line. It should be noted that the wet edge being parallel to the NIR axis in the new formulation is just a data-driven finding, rather than based on an established physical theory. Furthermore, the approximation of the soil moisture isolines with a quadratic function is introduced here only for the sake of simplicity. More complex and rigorous mathematical formulations for the soil isolines have been derived analytically by Taniguchi, Obata, and Yoshioka (2014, 2016).

3. Materials and methods

We evaluated the performance of both the CRN and new TRN models for the Salman Farsi Agro Industry sugarcane fields in Ahvaz, Iran (31.31 N, 48.67 E). Reference in situ soil moisture data was obtained at 22 locations within the field at 1, 5, 10, 30, and 60 cm depths via core sampling and oven-drying. Soil in this area is mostly medium- and fine-textured. Soil samples were collected from different soil textures within the study area.

Twelve cloud-free Landsat-8 images were acquired during the sugarcane growth season (April to October 2016). Atmospheric corrections were performed using parameters obtained from the metadata and data collected at the nearest weather station. Image radiometric calibration was performed to convert the pixel digital number to radiance to the top-of-atmosphere reflectance following USGS (2016). Image analysis was performed with the ERDAS Imagine 2014 software package (Hexagon Geospatial, Madison, AL, USA).

The CRN model, Equation (4), and new TRN model, Equation (10), were used to map soil saturation degree, W , based on the pixel distribution within the Red-NIR space. We determined the model parameters (i.e. M , D_{\max} and D_{\min} for the conventional model and a_{\max} for the new model) individually for each image. The correlation of W with the ground-measured soil moisture at different depths was compared with both methods. Steps for calculating saturation degree based on Landsat-8 observations with new and conventional methods are illustrated in Figure 3.

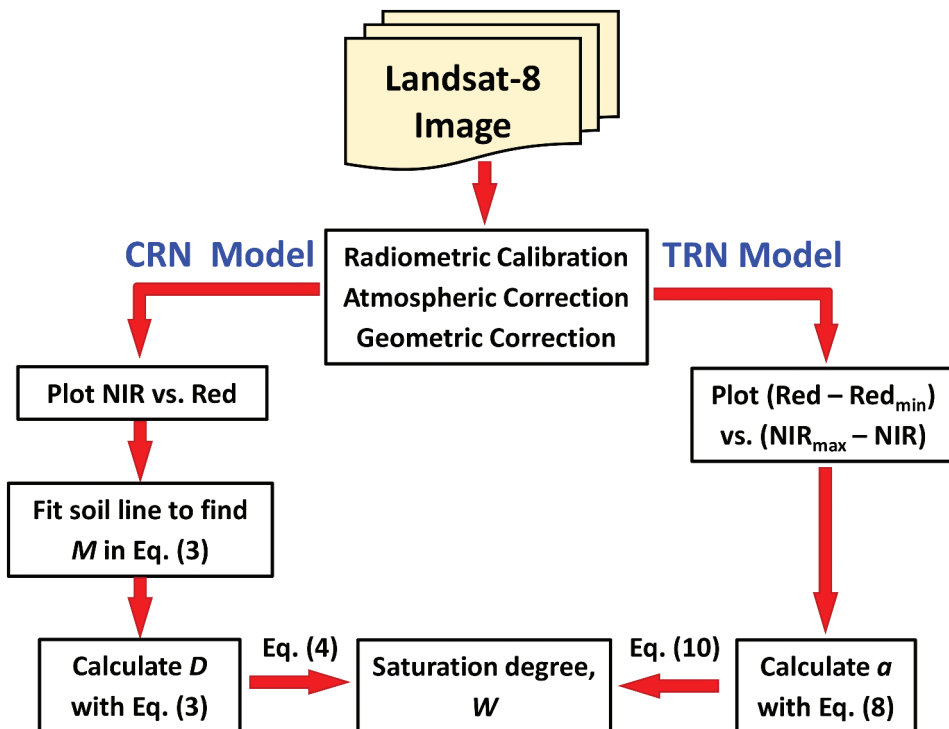


Figure 3. Flowchart illustrating steps for mapping soil saturation degree, W , based on Landsat-8 observations for the conventional Red-NIR (CRN) and Transformed Red-NIR (TRN) models.

4. Results and discussion

The pixel distribution in the TRN coordinate system at four sampling dates is presented in Figure 4. As shown, the geometry for all dates closely resembles a triangular space. The bare soil edge is nearly linear, while the dry and wet edges are nearly quadratic. This highlights that the soil moisture isolines defined with the new TRN model are more consistent with the observations than the isolines obtained with the CRN model.

As indicated above, calculating soil moisture based on the new TRN model only requires the coordinates of the full vegetation cover point (Red_{\min} , NIR_{\max}) based on which the sole parameter of the new model, a_{\max} in Equation (9), is calculated. Values of Red_{\min} and NIR_{\max} for different Landsat-8 observations are listed in Table 1. A slight temporal variability is observed for these values which reflects the temporal variability of the fractional vegetation cover during the sugarcane growth season.

The similarity of the triangular geometry at different dates observed in Figure 4 implies that a universal model parameterization (i.e. an invariant a_{\max} for a given study area) may be feasible, which potentially further increases the computational efficiency when numerous observations for the same location need to be analysed. The invariance of the Red-NIR space with respect to time reflects the invariance of the soil moisture–reflectance relationship. This is considered to be one major

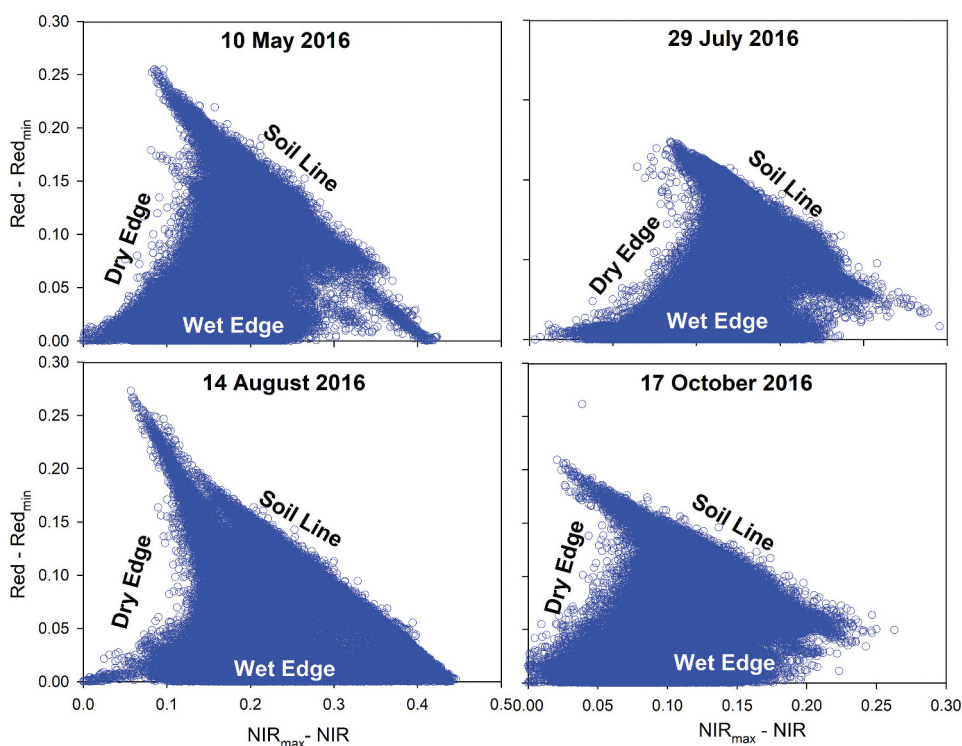


Figure 4. Pixel distribution within the proposed Red-NIR space.

Table 1. Original coordinates of the full vegetation cover point for various analysed Landsat-8 observations.

Date	Red _{min}	NIR _{max}
24 April 2016	0.129	0.448
10 May 2016	0.073	0.504
26 May 2016	0.087	0.522
11 June 2016	0.104	0.546
27 June 2016	0.098	0.548
13 July 2016	0.131	0.656
29 July 2016	0.108	0.638
14 August 2016	0.100	0.560
30 August 2016	0.108	0.560
15 September 2016	0.076	0.517
1 October 2016	0.074	0.388
17 October 2016	0.074	0.388

advantage of optical models when compared to the thermal models, as discussed in Sadeghi et al. (2017).

Correlations of the estimated normalized soil moisture values obtained with the conventional and new model with measured soil moisture at different depths are depicted in Figure 5. Note that the presented results have not been calibrated with ground reflectance data, i.e. the normalized soil moisture data were solely obtained from RS observations. As observed, the correlations are significantly improved with the new Red-NIR model, especially at and near the soil surface. The observed weak correlations of the CRN model can be partially explained by its two major limitations discussed earlier: (i) uncertainty of the soil line location due to soil spatial variability and (ii) inconsistency of the presumed soil moisture isolines with the actual Red-NIR space geometry. The estimation errors remaining in the TRN model can be attributed to the introduced simplifications such as the mismatch between the modelled and true soil moisture isolines as well as the saturation of visible signals at high soil moisture contents documented, for example, in Sadeghi, Jones, and Philpot (2015). Note that despite the discussed advantages of the TRN model it may be less efficient than the CRN model in capturing the field-to-field soil variability. This is because the soil line that is eliminated from the TRN model implicitly accounts for soil spatial variability through its effects on the soil moisture isolines (Taniguchi, Obata, and Yoshioka 2014, 2016).

Our results in Figure 5 indicate that surface data have the strongest correlations with these optical observations and the correlations consistently decrease as soil depth increases. These results also show a high gradient of soil moisture along the soil profile, as the correlation between moisture content at the surface and deeper layers is generally weak. This trend can be explained by the shallow penetration depth of visible and NIR electromagnetic radiation. Our results are in agreement with Carlson's (2013) intuition that '*it is not possible with optical measurements to determine deep layer soil water content*'. Our results, however, disagree with Zhan et al. (2007) who found 10 cm and 5 cm, respectively, as the effective soil depth for visible/NIR remote sensing of soil moisture. This contradiction in different studies has been discussed by Mahmood and Hubbard (2007).

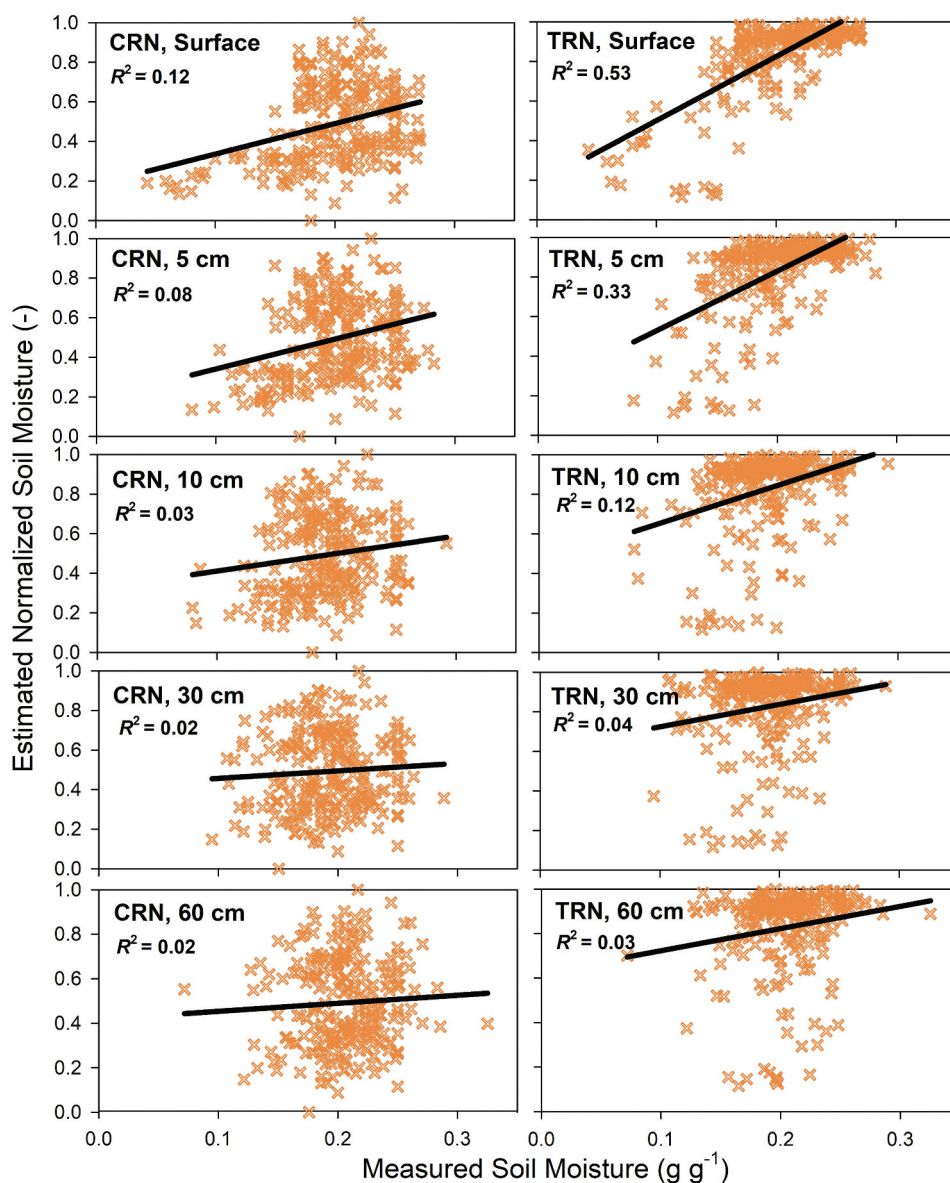


Figure 5. Estimated normalized soil moisture versus measured soil moisture from the conventional Red-NIR (CRN) and transformed Red-NIR (TRN) models. The coefficient of determination is denoted by R^2 .

To evaluate the significance of improvements introduced with the new TRN model, a one-way ANOVA analysis was performed. Accordingly, it was found that the difference between the CRN and TRN models was statistically significant with 99% level of confidence in 0-, 5-, 10-, and 30-cm depth and 95% level of confidence in 60-cm depth. This verifies that the new TRN model yields significantly more accurate estimates of soil moisture when compared to CRN, while, in addition, it is computationally more efficient than the CRN model.

Sample surface soil moisture maps generated with both models based on Landsat-8 images for June, July, and September 2016 are shown in [Figure 6](#). As evident, the soil moisture range in the maps generated with the new TRN model is generally higher than the range yielded by the CRN model. In the studied sugarcane field, each plot is surrounded by a dirt road, which probably represents dry bare soil at the time of imaging, due to the fact that the study area is located in an arid environment and that these roads are not irrigated. As evident from [Figure 6](#), the roads are more pronounced in the TRN maps than in the CRN maps, suggesting that the TRN maps are more realistic than the CRN maps.

The new TRN model has the two main advantages over the widely applied thermal triangle/trapezoid models as pointed out in Sadeghi et al. (2017): (i) it can be applied to satellites without thermal bands (e.g. Sentinel-2); and (ii) it can be universally parameterized for a given location. The new TRN model benefits from more readily available visible and NIR observations and can be applied to a broader range of satellite- and UAV-mounted sensors than the optical trapezoid model (OPTRAM) of Sadeghi et al. (2017). It additionally does not suffer from the high sensitivity of the SWIR band to oversaturated pixels, and hence, is computationally less demanding than the OPTRAM.

5. Summary and conclusions

In this paper, we introduced a simple, yet an efficient new model for estimation of soil moisture from the Red-NIR space. This work was motivated by the fact that visible and NIR observations are provided by most satellites and relatively inexpensive UAV-mounted cameras. The model provides a new index, i.e. parameter a defined in [Equation \(8\)](#), that is inversely correlated with soil moisture. The new Transformed Red-NIR (TRN) model is more accurate than the Conventional Red-NIR (CRN) model when comparing estimates of soil moisture from Landsat-8 observations with ground reference measurements. The TRN model is also simpler to apply than the CRN model as it does not require determination of the bare soil line. Unlike similar thermal and optical triangle/trapezoid models, the new TRN model does not need determination of the wet and dry edges. Both the CRN and TRN models' outputs were better correlated with surface soil moisture than the root-zone soil moisture.

The proposed model was tested here based on limited observations obtained from a sugarcane field in southwestern Iran. Future research is needed to more comprehensively evaluate this model for other geographical locations with different soil and landcover types. Although the proposed model advances the CRN approach, its estimates are still subject to errors due to the simplifying model assumptions such as the mismatch between the presumed and true soil moisture isolines. Future modifications of the model to formulate more realistic and physically consistent soil moisture isolines may further improve the accuracy of the Red-NIR approach to remote sensing of soil moisture.

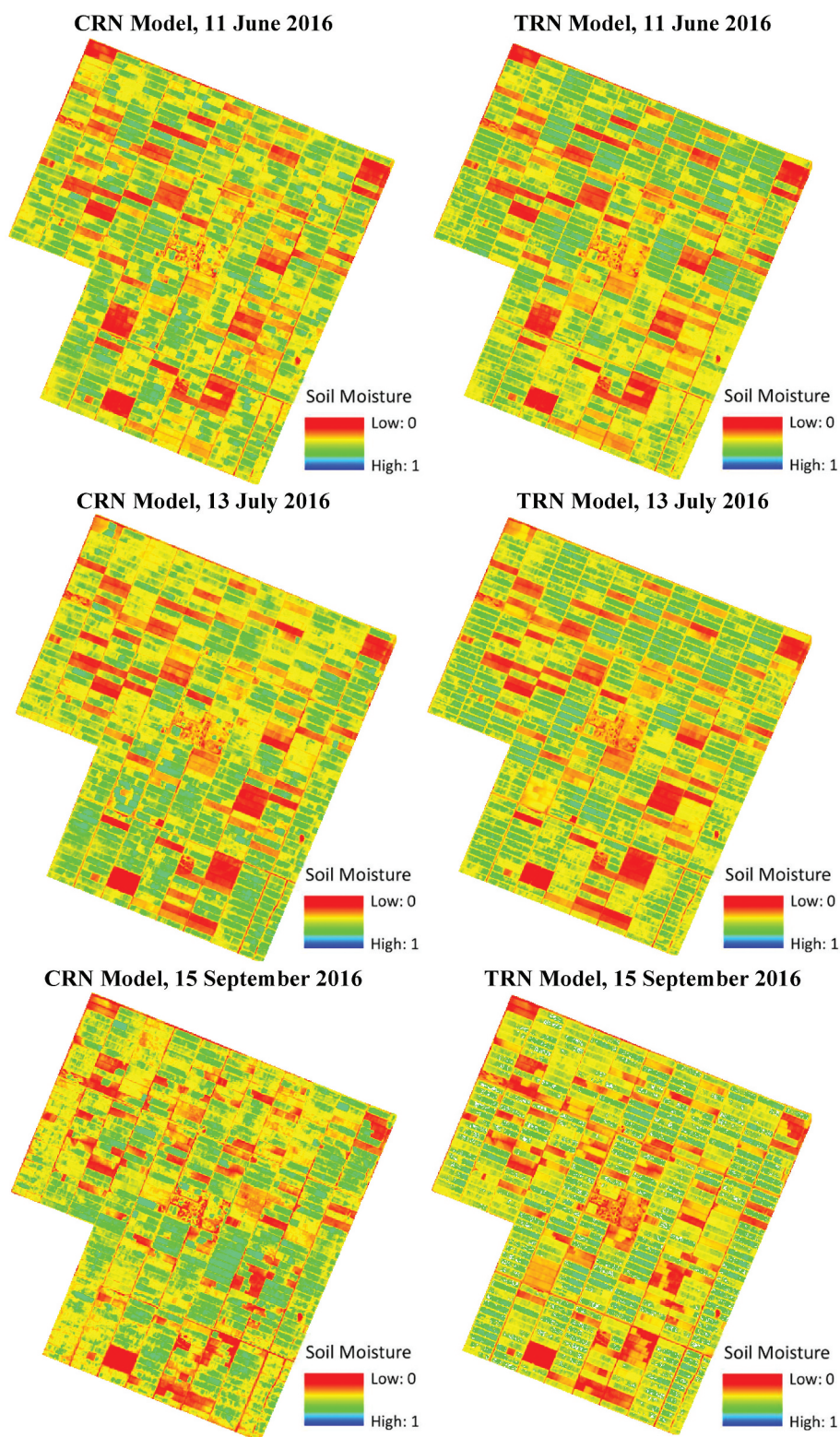


Figure 6. Soil moisture maps generated with the conventional Red-NIR (CRN) and transformed Red-NIR (TRN) models.

6. Geolocation information

The Salman Farsi Agro-Industry sugarcane fields are located in Ahvaz province in south-western Iran between latitudes 31° 00' 30" and 32° 30' 00" N and longitudes 48° 15' 00" and 48° 40' 40" E.

Acknowledgements

We appreciate the support of the Salman Farsi Sugarcane Farming and Industrial staff with the field work and ground measurements.

Disclosure statement

No potential conflict of interest was reported by the authors.

Funding

This work was supported by National Science Foundation (NSF) grants no. 1521469 and 1521164 and by the United States Department of Agriculture (USDA) National Institute of Food and Agriculture (NIFA), Hatch/Multi-State project number UTAO+1477. Additional support was provided by the Utah Agricultural Experiment Station (UAES), Utah State University, approved as UAES journal paper no. 9351.

References

- Amani, M., S. Parsian, S. M. MirMazloumi, and O. Aieneh. 2016. "Two New Soil Moisture Indices Based on the NIR-red Triangle Space of Landsat-8 Data." *International Journal of Applied Earth Observation and Geoinformation* 50: 176–186. doi:10.1016/j.jag.2016.03.018.
- Atzberger, C., and K. Richter. 2012. "Spatially Constrained Inversion of Radiative Transfer Models for Improved LAI Mapping from Future Sentinel-2 Imagery." *Remote Sensing of Environment* 120: 208–218. doi:10.1016/j.rse.2011.10.035.
- Babaeian, E., M. Sadeghi, T. E. Franz, S. Jones, and M. Tuller. 2018. "Mapping Soil Moisture with the OPTical TRapezoid Model (OPTRAM) Based on Long-term MODIS Observations." *Remote Sensing of Environment* 211: 425–440. doi:10.1016/j.rse.2018.04.029.
- Babaeian, E., M. Sadeghi, S. B. Jones, C. Montzka, H. Vereecken, and M. Tuller. 2019a. "Ground, Proximal, and Satellite Remote Sensing of Soil Moisture." *Reviews of Geophysics* 57 (2): 530–616. doi:10.1029/2018RG000618.
- Babaeian, E., P. Sidike, M. S. Newcomb, M. Maimaitijiang, S. A. White, J. Demieville, ... V. Sagan. 2019b. "A New Optical Remote Sensing Technique for High-Resolution Mapping of Soil Moisture." *Frontiers in Big Data* 2: 37.
- Carlson, T. N. 2013. "Triangle Models and Misconceptions." *International Journal of Remote Sensing Applications* 3 (3): 155–158.
- Carlson, T. N., R. R. Gillies, and E. M. Perry. 1994. "A Method to Make Use of Thermal Infrared Temperature and NDVI Measurements to Infer Surface Soil Water Content and Fractional Vegetation Cover." *Remote Sensing Reviews* 9 (12): 161–173. doi:10.1080/02757259409532220.
- Chen, N., Y. He, and X. Zhang. 2017. "Nir-red Spectra-based Disaggregation of Smap Soil Moisture to 250 M Resolution Based on Oznet in Southeastern Australia." *Remote Sensing* 9 (1): 51. doi:10.3390/rs9010051.
- Crow, W. T., E. Han, D. Ryu, C. R. Hain, and M. C. Anderson. 2017. "Estimating Annual Water Storage Variations in Medium-scale (2000–10 000 Km²) Basins Using Microwave-based Soil

- Moisture Retrievals." *Hydrology and Earth System Sciences* 21 (3): 1849–1862. doi:[10.5194/hess-21-1849-2017](https://doi.org/10.5194/hess-21-1849-2017).
- Entekhabi, D., E. G. Njoku, P. E. O'Neill, K. H. Kellogg, W. T. Crow, W. N. Edelstein, ... J. Kimball. 2010. "The Soil Moisture Active Passive (SMAP) Mission." *Proceedings of the IEEE* 98 (5): 704–716. doi:[10.1109/JPROC.2010.2043918](https://doi.org/10.1109/JPROC.2010.2043918).
- Ghulam, A., Z. L. Li, Q. Qin, H. Yimit, and J. Wang. 2008. "Estimating Crop Water Stress with ETM+ NIR and SWIR Data." *Agricultural and Forest Meteorology* 148 (11): 1679–1695. doi:[10.1016/j.agrformet.2008.05.020](https://doi.org/10.1016/j.agrformet.2008.05.020).
- Ghulam, A., Q. Qin, T. Teyip, and Z. L. Li. 2007. "Modified Perpendicular Drought Index (MPDI): A Real-time Drought Monitoring Method." *ISPRS Journal of Photogrammetry and Remote Sensing* 62 (2): 150–164. doi:[10.1016/j.isprsjprs.2007.03.002](https://doi.org/10.1016/j.isprsjprs.2007.03.002).
- Hassan-Esfahani, L., A. Torres-Rua, A. Jensen, and M. McKee. 2015. "Assessment of Surface Soil Moisture Using High-resolution Multi-spectral Imagery and Artificial Neural Networks." *Remote Sensing* 7 (3): 2627–2646. doi:[10.3390/rs70302627](https://doi.org/10.3390/rs70302627).
- Kerr, Y. H., P. Waldteufel, J. P. Wigneron, J. A. M. J. Martinuzzi, J. Font, and M. Berger. 2001. "Soil Moisture Retrieval from Space: The Soil Moisture and Ocean Salinity (SMOS) Mission." *IEEE Transactions on Geoscience and Remote Sensing* 39 (8): 1729–1735. doi:[10.1109/36.942551](https://doi.org/10.1109/36.942551).
- Mahmood, R., and K. G. Hubbard. 2007. "Relationship between Soil Moisture of near Surface and Multiple Depths of the Root Zone under Heterogeneous Land Uses and Varying Hydroclimatic Conditions." *Hydrological Processes: An International Journal* 21 (25): 3449–3462. doi:[10.1002/hyp.6578](https://doi.org/10.1002/hyp.6578).
- Mananze, S., I. Pôças, and M. Cunha. 2019. "Agricultural Drought Monitoring Based on Soil Moisture Derived from the Optical Trapezoid Model in Mozambique." *Journal of Applied Remote Sensing* 13 (2): 024519. doi:[10.1117/1.JRS.13.024519](https://doi.org/10.1117/1.JRS.13.024519).
- Mobasheri, M. R., and M. Amani. 2016. "Soil Moisture Content Assessment Based on Landsat 8 Red, Near-infrared, and Thermal Channels." *Journal of Applied Remote Sensing* 10 (2): 026011. doi:[10.1117/1.JRS.10.026011](https://doi.org/10.1117/1.JRS.10.026011).
- Moran, M. S., T. R. Clarke, Y. Inoue, and A. Vidal. 1994. "Estimating Crop Water Deficit Using the Relation between Surface-air Temperature and Spectral Vegetation Index." *Remote Sensing of Environment* 49 (3): 246–263. doi:[10.1016/0034-4257\(94\)90020-5](https://doi.org/10.1016/0034-4257(94)90020-5).
- Richardson, A. J., and C. L. Wiegand. 1977. "Distinguishing Vegetation from Soil Background Information." *Photogrammetric Engineering and Remote Sensing* 43 (12): 1541–1552.
- Robinson, D. A., C. S. Campbell, J. W. Hopmans, B. K. Hornbuckle, S. B. Jones, R. Knight, O. Wendroth, J. Selker, and O. Wendroth. 2008. "Soil Moisture Measurement for Ecological and Hydrological Watershed-scale Observatories: A Review." *Vadose Zone Journal* 7 (1): 358–389. doi:[10.2136/vzj2007.0143](https://doi.org/10.2136/vzj2007.0143).
- Sadeghi, M., E. Babaeian, M. Tuller, and S. B. Jones. 2017. "The Optical Trapezoid Model: A Novel Approach to Remote Sensing of Soil Moisture Applied to Sentinel-2 and Landsat-8 Observations." *Remote Sensing of Environment* 198: 52–68. doi:[10.1016/j.rse.2017.05.041](https://doi.org/10.1016/j.rse.2017.05.041).
- Sadeghi, M., A. Ebtehaj, W. T. Crow, L. Gao, A. J. Purdy, J. B. Fisher, S. B. Jones, E. Babaeian, and M. Tuller. 2019. "Global Estimates of Land Surface Water Fluxes from SMOS and SMAP Satellite Soil Moisture Data." *Journal of Hydrometeorology* 21: 241–253. doi:[10.1175/JHM-D-19-0150.1](https://doi.org/10.1175/JHM-D-19-0150.1).
- Sadeghi, M., S. B. Jones, and W. D. Philpot. 2015. "A Linear Physically-based Model for Remote Sensing of Soil Moisture Using Short Wave Infrared Bands." *Remote Sensing of Environment* 164: 66–76. doi:[10.1016/j.rse.2015.04.007](https://doi.org/10.1016/j.rse.2015.04.007).
- Shafian, S., and S. Maas. 2015. "Index of Soil Moisture Using Raw Landsat Image Digital Count Data in Texas High Plains." *Remote Sensing* 7 (3): 2352–2372. doi:[10.3390/rs70302352](https://doi.org/10.3390/rs70302352).
- Sun, H. 2015. "Two-stage Trapezoid: A New Interpretation of the Land Surface Temperature and Fractional Vegetation Coverage Space." *IEEE Journal of Selected Topics in Applied Earth Observations and Remote Sensing* 9 (1): 336–346. doi:[10.1109/JSTARS.2015.2500605](https://doi.org/10.1109/JSTARS.2015.2500605).
- Taniguchi, K., K. Obata, and H. Yoshioka. 2014. "Derivation and Approximation of Soil Isoline Equations in the Red-near-infrared Reflectance Subspace." *Journal of Applied Remote Sensing* 8 (1): 083621. doi:[10.1117/1.JRS.8.083621](https://doi.org/10.1117/1.JRS.8.083621).

- Taniguchi, K., K. Obata, and H. Yoshioka. 2016. "Soil Isoline Equations in the red–NIR Reflectance Subspace Describe a Heterogeneous Canopy." *Journal of Applied Remote Sensing* 10 (1): 016013. doi:[10.1117/1.JRS.10.016013](https://doi.org/10.1117/1.JRS.10.016013).
- Yin, Z., T. Lei, Q. Yan, Z. Chen, and Y. Dong. 2013. "A Near-infrared Reflectance Sensor for Soil Surface Moisture Measurement." *Computers and Electronics in Agriculture* 99: 101–107. doi:[10.1016/j.compag.2013.08.029](https://doi.org/10.1016/j.compag.2013.08.029).
- Zhan, Z., Q. Qin, A. Ghulan, and D. Wang. 2007. "NIR-red Spectral Space Based New Method for Soil Moisture Monitoring." *Science in China Series D: Earth Sciences* 50 (2): 283–289. doi:[10.1007/s11430-007-2004-6](https://doi.org/10.1007/s11430-007-2004-6).